Chapter – 2

EXPERIMENTAL PROCEDURE

2.1 Material

A low carbon steel (LCS) of chemical composition C-0.08wt.%, Mn-0.31wt.%, P-0.031 wt.%, S-0.01 wt.%, Si-0.091 wt.%, Al-0.035 wt.%, and balance Fe was used in the present investigation. The steel plates of 330 x 220 x 38 mm^3 size were procured from Research and Development Center for Iron and Steel (RDCIS), Steel Authority of India Ltd (SAIL), Ranchi, India. The workpieces of 15-mm diameter and 80-mm length were machined from hot-rolled plates in the rolling direction.

2.2 Equal-Channel Angular Pressing

Low carbon steel workpieces were deformed by equal-channel angular pressing using a die (shown in Figure 2.1(a)). The die was made up of die steel H11, of hardness ~ HRC 55. The workpieces were deformed by ECAP at room temperature (27°C) using route Bc (rotating the workpiece 90° anticlockwise about the pressing axis between the two consecutive passes) [Furukwa et al. 1998] by a hydraulic press of 30 ton capacity with a ram speed of 60 mm/min. The die was lubricated by molybdenum disulfide (MoS_2) with high-density paraffin liquid to reduce friction between the die and the workpiece. No back pressure was used during equal-channel angular pressing. However, some amount of friction between die and workpiece acts as back pressure. The two channels of 15-mm diameter intersecting at an inner

intersection angle (φ) of 120° and an outer arc angle of (Ψ) 60° were used in the die. The imposed shear strain can be calculated by Equation (2.1).

$$\gamma = 2\cot\left(\frac{\Phi}{2} + \frac{\Psi}{2}\right) + \Psi\operatorname{cosec}\left(\frac{\Phi}{2} + \frac{\Psi}{2}\right) \quad (2.1)$$

where φ, and Ψ are in radians.

Every passage of the work piece through the channel introduces a shear strain of 1 or von Mises' equivalent strain (ε_{vm}) of 0.6. The imposed equivalent strain (ε_{vm}) is accumulative and can be calculated for N number of passes by the following equation (2.2) [Iwahashi et al. 1996].

$$\varepsilon_{vm} = \frac{\gamma N}{\sqrt{3}} \quad (2.2)$$

The exit channel of the equal-channel angular pressing die was 0.2 mm lesser than the inlet channel to accommodate elastic recovery. The pressed workpiece and reference directions are shown in Figure 2.1 (b). The workpiece after every pressing was cleaned for burs by emery papers. In this thesis work, workpieces were deformed to a maximum equivalent strain (ε_{vm}) of 16.8 (28 passes). After ε_{vm} = 16.8 hairline cracks appeared at the inner side close to the shear plane. Therefore, the ECAP of selected low carbon steel was carried out only upto ε_{vm} = 16.8. To avoid the end effect, 20 mm length pieces from both the ends of the workpiece were cut off and the central part of the workpiece was characterized.

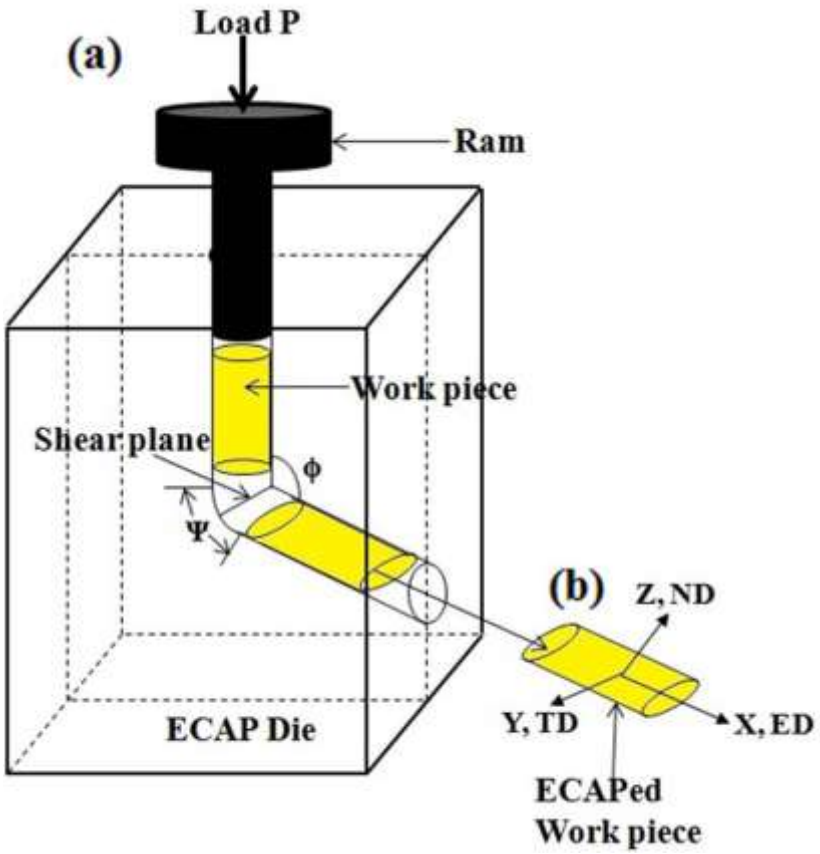

Figure 2.1: Schematic diagram of (a) ECAP die assembly with work piece, (b) ECAPed workpiece with reference directions, X, Y, Z or ED, TD and ND respectively.

The extrusion direction (ED), transverse direction (TD), and normal direction (ND) are represented by X, Y, and Z directions respectively. The X, Y, and Z planes are perpendicular to X, Y, and Z directions. The deformed workpieces (Figure 2.1(b)) were sectioned along the flow plane or Y-plane for characterisation, whereas X-plane was the transverse plane perpendicular to the extrusion direction. The Y-plane was the flow plane vertical to the extruded workpiece, and Z-plane was the horizontal but parallel to the top surface along the extrusion direction. The ECAPed samples were designated as ECAP-ε_{vm}, where ε_{vm} indicated the amount of equivalent strain. The designation of ECAPed samples is given in Table 2.1.

Table 2.1: Designations of as-received and ECAPed low carbon steel samples.

Sr.No	Number of passes	Equivalent Strain (ε_{vm})	Designation of ECAPed samples (ECAP-ε_{vm})
1	0	0	ECAP-0
2	1	0.6	ECAP-0.6
3	2	1.2	ECAP-1.2
4	3	1.8	ECAP-1.8
5	5	3	ECAP-3
6	10	6	ECAP-6
7	15	9	ECAP-9
8	20	12	ECAP-12
9	28	16.8	ECAP-16.8

As far as post-ECAP processing is concerned, the ECAP-12 plates were further rolled at room temperature (cold rolling) on Y-plane and in X-direction (Figure 2.2) for 80% reduction in area (the samples were designated as ECAP-12-CR80 (Table 2.2)), and ECAP-16.8 plates were chosen for rolling at 223 K (-50°C) (cryo-rolling) for 75% reduction in area (the samples were designated as ECAP-16.8-CRR75 (Table 2.2)). The subzero temperature was maintained by mixing liquid nitrogen in ethanol and temperature was continuously measured by calibrated Fe-constantan thermocouple.

Table 2.2: Designation of samples of ECAP followed by cold-rolling or cryo-rolling.

Sr. No.	Sample Details	Designation
1	ECAP upto ε_{vm}=12 and Coldrolled for 80% reduction in area	ECAP-12-CR-80
2	ECAP upto ε_{vm}=16.8 and Cryo rolled for 75% reduction in area	ECAP-16.8-CRR-75

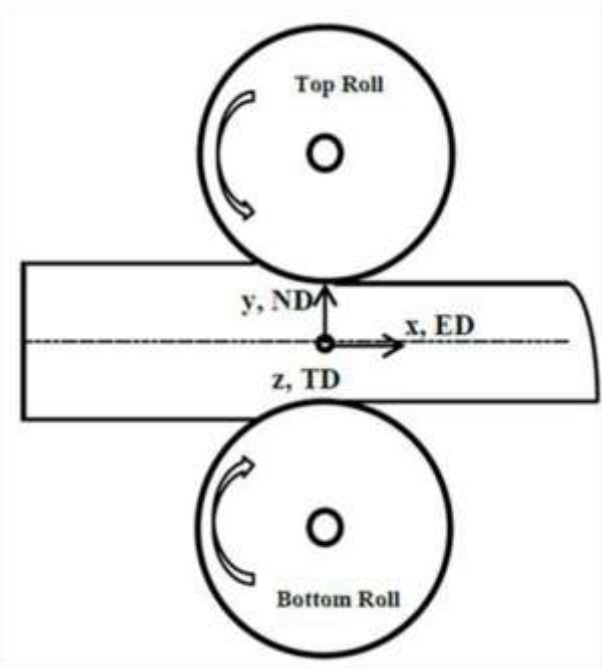

Figure 2.2: Schematic diagram of cold-rolling/cryo-rolling of the equal-channel angular pressed workpiece with extrusion direction (ED, parallel to X), normal direction (parallel to Y), and transverse direction (TD, parallel to Z) designated.

Samples subjected to cold rolling after ECAP were flash annealed for 5 minutes in molten $NaNO_3$ salt, maintained at 580°C and 600°C temperature as two sets. The flash annealed samples were quenched in water at room temperature as two sets. The cold-rolled and flash annealed specimens were designated as ECAP-12-CR80-FAT. the cryo-rolled and flash-annealed workpieces were designated as ECAP-16.8-CRR-75-FAT, where T was flash annealing temperature for both the cases (Table 2.3). The cryo-rolled samples were flash-annealed at 475°C-675°C to identify the suitable temperature for secondary recrystallisation, and the annealed samples were quenched in the same way as above for cooling of flash annealed cold-rolled samples.

Table 2.3: Designation of low carbon steel specimen after ECAP followed by cold-rolling or cry-rolling, and flash annealing.

Sr. No.	Sample details	Designation
1	ECAP-12-CR-80 and flash annealing at 580°C	ECAP-12-CR-80FA580
2	ECAP-12-CR-80 and flash annealing at 600°C	ECAP-12-CR-80FA600
3	ECAP-16.8-CRR-75 and flash annealed at 475°C	ECAP-16.8-CRR-75FA475
4	ECAP-16.8-CRR-75 and flash annealed at 500°C	ECAP-16.8-CRR-75FA500
5	ECAP-16.8-CRR-75 and flash annealed at 550°C	ECAP-16.8-CRR-75FA550
6	ECAP-16.8-CRR-75 and flash annealed at 575°C	ECAP-16.8-CRR-75FA575
7	ECAP-16.8-CRR-75 and flash annealed at 600°C	ECAP-16.8-CRR-75FA600
8	ECAP-16.8-CRR-75 and flash annealed at 625°C	ECAP-16.8-CRR-75FA625
9	ECAP-16.8-CRR-75 and flash annealed at 650°C	ECAP-16.8-CRR-75FA650
10	ECAP-16.8-CRR-75 and flash annealed at 675°C	ECAP-16.8-CRR-75FA675

2.3 Characterisation of Ultrafine-grained Low Carbon Steel

Low carbon steel samples were taken for various microstructural characterisation from the center of the ECAPed workpiece as shown in Figure 2.3. Microstructural characterisation of ECAPed samples was performed on Y-plane but rolled samples were analyzed on rolling plane. Microstructures of low carbon steel were studied by optical microscopy (OM), scanning electron microscopy (SEM), electron back scattered diffraction (EBSD) and transmission electron microscopy (TEM). Bulk and microtexture were investigated by X-ray diffraction and EBSD respectively. Mechanical properties were evaluated by hardness measurements and tensile testing. Fractured surfaces of tensile tested samples were investigated by SEM.

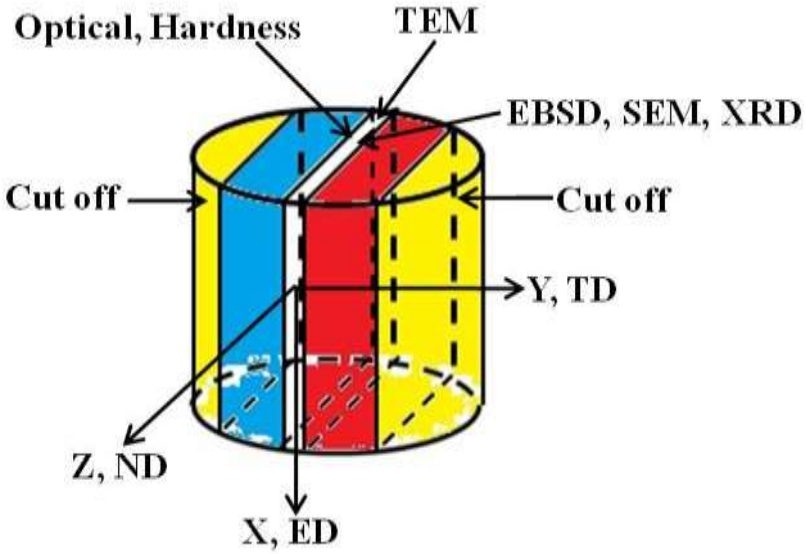

Figure 2.3: Location of samples taken for various microstructural investigations.

2.3.1 Optical Microscopy

The metallographic samples (Figure 2.3) were ground using coarse to fine abrasive papers and finally polished using fine alumina powder. The polished samples were etched in 2% nital solution to reveal the microstructure. The etched samples were studied by Metalux-3 optical microscope. The grain size was measured on micrographs by the Heyn's linear intercept method.

2.3.2 Scanning Electron Microscopy

Rectangular samples of 15 x 10 x 5.5 mm^3 and 10 x 10 mm^2 were cut from ECAPed workpieces at the Y-plane and from rolled samples. Microstructures were studied by FEI Quanta 200 FEG scanning electron microscope (SEM) operating at 20 kV, and working distance of 15 mm. Ferritic grain size distributions and pearlitic structure were investigated.

2.3.3 Electron Back Scattered Diffraction (EBSD)

Samples of 10 x 10 x 5 mm^3 were cut from the ECAPed workpiece at Y-plane (Figure 2.4) and specimen of 10 x10 x 1.5-2 mm^3 was sectioned from rolled sheets on rolling plane. Both types of samples were mechanically ground and polished with alumina and colloidal silica abrasives. The mechanically polished samples were electropolished at 278K (5ºC), 35 V for 20 seconds. Electropolished samples were scanned for electron back scattered diffraction study in FEI NovaNano450 scanning electron microscope (SEM). The samples were scanned at an operating voltage of 20 kV, probe current of 16 to 23 nA, and a working distance of 15 mm. Scan areas of 250 x 250 μm^2 and 105 x 105 μm^2 were taken for ε_{vm}=0 and ε_{vm}=0.6 respectively. Step size of 0.1 μm and 0.05 μm were chosen for ε_{vm} = 0 and 0.6 respectively. For ECAPed sample of ε_{vm}=1.2 to 16.8, a scan area of 65 x 65 μm^2 and a step size of 0.05 μm were selected. In terms of data points the scan area all together ranges from 1.1-2.0 million. An indexing rate of 154 fps was achieved. Scanned EBSD data was analyzed by TSL (TexSemLab) 5.1 Software for image quality map, grain boundary angle and its fraction, and misorientation angle. Misorientation angle of 2º to 15º and 15º to 180º were assigned to low angle grain boundaries (LAGBs) and high angle grain boundaries (HAGBs) respectively.

2.3.4 Transmission Electron Microscopy

Slices of 200 μm thickness were cut at Y-plane at the center of the pressed workpiece. The samples were ground by emery papers with 50 micron thin foils, and 3 mm discs were punched from the foils. The discs were electropolished by FISCHIONE twin jet polisher (model 120) at 22 V using electrolyte of 95% methanol and 5% perchloric acid maintained at 233K (-40ºC). Detailed microstructure, defects,

and grain boundaries were studied by transmission electron microscopy (TEM) (Tecnai 20G^2) operating at 200 kV.

2.3.5 X-ray Diffraction

Low carbon steel samples (Figure 2.3), were also scanned by a Bruker D8 Discover system of x-ray diffractometer operating at 50 kV voltage and current of 1000 µA. The as-received sample was annealed for 2 hours at 1253 K (980ºC) and cooled in the furnace and was assumed to be well-annealed material. The goodness of fit was 0.98. Scanning was done by varying the 2θ from 20° to 105° and step size of 0.05º. The scanned data of well-annealed material was utilized to correct instrument broadening. The OriginPro 8 software package was used to process the scanned data. Peaks were identified and fitted with a pseudo-Voigt (pV) function. A pV function was a linear combination of the Lorentzian (L), and the Gaussian (G) functions. Further analyses were carried out on the (1 1 0) plane for all the samples.

The Stibitz equation [Stibitz 1936, Hazra et al. 2009] was used to calculate the elastic stored energy(E_l) in (110) plane from X-ray diffraction measurement.

$$E_l = \frac{3}{2} E \frac{\left(\frac{\delta d}{d}\right)^2}{1+2\nu^2} \qquad (2.3)$$

Where, d was interplanar spacing, δd was the change in interplanar spacing, and the ratio δd /d could be calculated by Equation 2.4.

$$\frac{\delta d}{d} = \frac{\sqrt{I^2 - I_0^2}}{2tan\theta} \qquad (2.4)$$

Here, Γ was full width at half maximum (FWHM), and Γ_0 was FWHM of well-annealed material. FWHM was determined from Pseudo-Voigt fit on experimented data. Young's modulus (E) for [110] directions is 221 GPa [Borbely et al. 2000]. Poisson's ratio (ν) is taken as 0.3 and molar volume of iron is 7.11 cc/mole.

Crystallite size and microstrain were determined from the (110) reflection using the corrected Lorentzian and the Gaussian components respectively. The corrected Lorentzian (L) component of the integral breadth β'_L was separated from instrumental breadth using the following relation.

$$\beta'_L = \beta_L - \beta_{L0} \tag{2.5}$$

Where β_{L0} was the Lorentzian component of the integral breadth of well-annealed material. β_L was a Laurentzian component of the integral breadth of the sample. The corrected (for instrumental broadening) Gaussian component (β'_G) of the integral breadth was extracted from the Gaussian component (β_G) using the following Equation.

$$\beta'^2_G = \beta_G^2 - \beta_{G0}^2 \tag{2.6}$$

Where β_{G0} was the Gaussian component of the integral breadth of well-annealed material. The average domain size (D) on (110) plane, and lattice strain (e_{110}) were calculated from the following relationship [Klug 1954].

$$D = \lambda/\beta'_L \cos\theta \quad (2.7)$$

$$e_{110} = \frac{\beta'_G}{4\tan\theta} \quad (2.8)$$

Where, θ was the Bragg angle, D was average domain size or crystallite size, λ was the wavelength of the X-ray radiation. The calculated strain value (e) was multiplied by 100 for percentage strain.

The dislocation density at (110) was calculated using crystallite size and microstrain using the equation (2.9) [Williamson et al. 1956, Smallman et al. 1957, Zhang et al. 1997] from the diffraction measurement.

$$\rho_{110} = (\rho_D \rho_S)^{1/2} = \frac{2\sqrt{3}\langle e^2_{110}\rangle^{1/2}}{D_{110} b} \quad (2.9)$$

where b is the Burger vector (0.248 nm for bcc metals).

2.3.6 Bulk texture

Samples of ECAP-0.6 to ECAP-16.8 and of size 10 x 10 x 5 mm^3 were scanned on Y-plane (Figures 2.3, 2.4), and ECAP-0 sample was scanned on RD-TD plane (Figure 2.2) for bulk texture measurement using PANalytical X_Pert PRO MRD system utilizing a Cu Kα radiation operating at an acceleration voltage of 45 kV and 40 mA current. The bulk texture is represented by pole figures (PFs) and orientation distribution functions (ODFs).

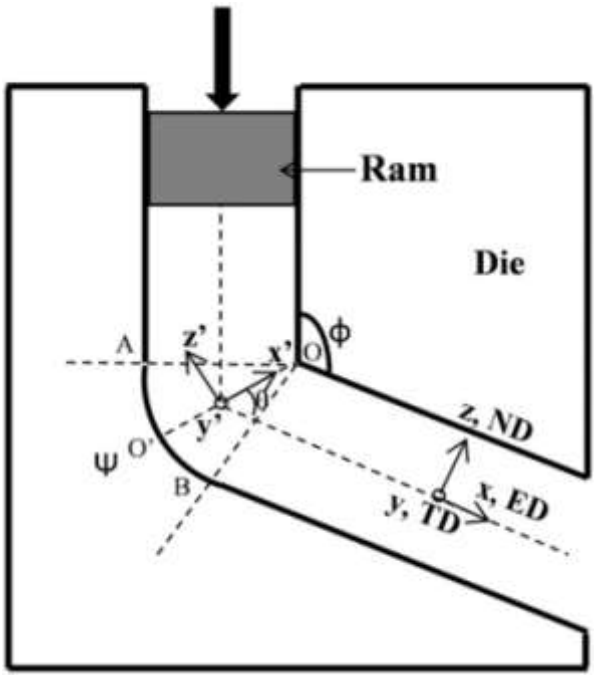

Figure 2.4: Schematic diagram of the ECAP die with sample directions and shear plane directions.

The [110] pole figures of as-received and equal-channel angular pressed samples were reported in this investigation, which were ND, and TD view for as-received and ECAPed samples respectively with orientation density contour levels of 0.8. 1, 1.3, 1.6, 2, 2.5, 3.2, 4, 5 and 6.4. The texture data were rotated by $\varphi 2 = 60°$ around TD to get the negative simple shear texture. Pole figures [100], [110], [112] and [103] were projected on TD plane.

The crystal coordinate system (Cc) is related to sample coordinate system (Cs) through orientation **g.**

$$Cc = g.Cs \qquad 2.10$$

The pole figure contains clear orientation information of the particular component in a single crystal. However, in the case of polycrystalline sample, orientation density was represented by the scattered distribution of each component.

The representation of simple shear texture in pole figure involves partial <111> and {110} fibers which were represented in (110) pole figure for 120° ECAE die. The components on the pole figure were rotated by 60° around TD for die having outer intersection angle of Φ~120° and resembles negative simple shear texture [Li et al. 2005]. Further analysis of the simple shear texture in the present investigation was done using the same standard pole figures for BCC material.

Since projection of 3D information on 2D projection plane or pole figure can lead to loss of information and uncertainty in data and also, there is overlapping of components in pole figures at some places, at least 4 pole figures are required to represent texture completely. There is a need for an alternative representation of texture.

In the present study the ODFs were extracted by using MTM-FHM software by inversion of 4 incomplete pole figures ((100), (110), (112) and (103)) [Houtte 2009] and contour density scale of 10 levels of density of 0.8, 1.2, 2.0, 3.0, 5, 7.5, 10, 13, 17, 20 are utilized. All ODFs were analyzed based on main ideal orientations in simple shear deformation of BCC materials as given by Li[a] at al. [Li[a] et al. 2005]. Ideal shear texture components of BCC material after one pass of ECAP, using a die of different inner intersection angle (φ), can be correlated with rotating texture components by φ/2 in negative simple shear about the normal direction of the sample [Li et al. 2007]. The ideal components of the material (as given by Li[a] et al. [Li[a] et al. 2005]) were rotated by φ/2=60° along φ_1 direction in the Eulers space to match with the components in ODFs of low carbon steel) subjected to one pass of ECAP using an

ECAP die of φ=120º and ψ=60º. The rotated ideal components were projected on φ_2=45º section of negative simple shear. ODFs of low carbon steel subjected to more than one pass adopting strain paths Bc after ECAP are produced in the present study to find the deviation of ideal components on equivalent strain as these deviations cannot be predicted due to rotation of samples around non-symmetric texture axis. The shear texture of low carbon steel is compared with published information of interstitial free steel processed at similar equivalent strain upto 15 [Verma[a] et al. 2016].

2.3.7 Micro Texture

For microtexture analysis, EBSD scanned data was examined using TSL (TexSem Lab) 5.1 software. The ODF plots were reported for the following: ECAP-0, ECAP-12, ECAP-12-CR-80, ECAP-12-CR-80FA580, and ECAP-12-CR-80FA600 samples contour levels of 0.656, 1, 1.523, 2.321, 3.535, 5.385, 8.203, 12.497, 19.037, 29.

2.4 Evaluation of Mechanical Properties

Tensile testing and Vickers microhardness measurements were carried out to evaluate the mechanical properties of low carbon steel samples under the chosen mechanical conditions.

2.4.1 Tensile Testing

Rod-shaped tensile samples of guage length 15 mm and guage diameter 4.5 mm were machined from as-received, and equal-channel angular pressed low carbon steel (Figure 2.9).

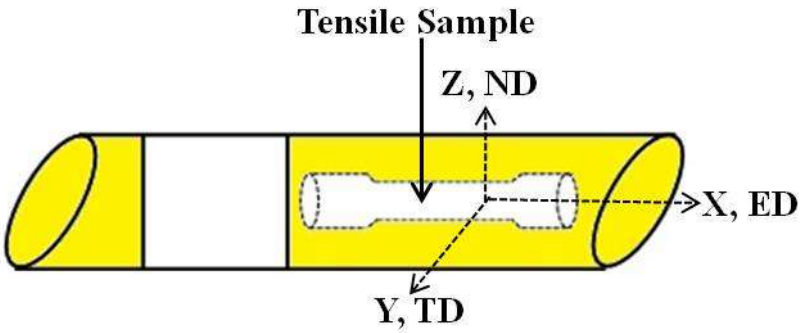

Figure 2.5: Orientation and location of tensile sample on equal-channel angular pressed workpiece.

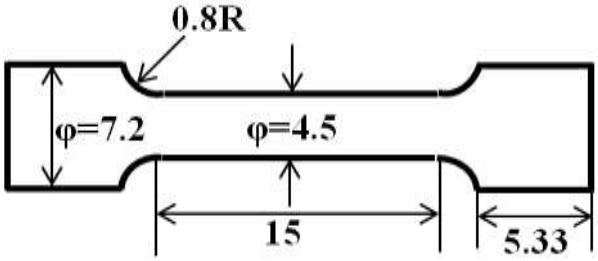

Figure 2.6: Typical dimensions of round tensile sample (all dimensions in mm).

Plate shaped tensile samples of guage length 15 mm and guage width 5 mm with a thickness of 1 mm were prepared [Hazra et al. 2011]. Tensile testing for the rod, as well as plate samples, was conducted using an Instron model 4201 at a crosshead speed of 1 mm per minute at room temperature. Engineering stress–engineering plastic strain, yield strength, ultimate tensile strength, uniform elongation, and total elongation were reported.

2.4.2 Hardness Measurement

The Vickers microhardness tests were performed at the various loads in the range of 10 gm to 2 kg for as-received low carbon steel. The minimum load for load independent hardness was found to be 100 gm. Therefore all other samples, i.e.,

ECAPed, rolled, and flash annealed samples were indented at 100 gm load to find the load independent hardness value. At least 20 measurements were taken at 980 mN load in the Y-plane of a sample, and an average hardness value with standard deviation was reported.

Hardness values were plotted against $d^{-1/2}$ where d is the average grain size. The hardness of the material was related to grain size through well known Hall-Petch [Hall 1951, Petch 1953] equation which is given by Equation 2.12.

$$H = Ho + \frac{K}{d^{1/2}} \qquad (2.12)$$

Where Ho is the hardness value of the single crystal and K was the gradient (constant) for polycrystalline coarse-grained material. Hall-Petch constants Ho, and K were calculated from a linear fit by the method of least square.

2.5 Fractography

Fracture surfaces of deformed and annealed low carbon steel tensile tested samples were examined by Quanta 200 FEG SEM. The average diameters of dimples were measured at 20 different locations of every fractograph, and standard deviation value was reported. The average dimple size and cleavage fracture area were reported. The average dimple size and stored energy were correlated.